PPPL-2490

DE #0457-X
PPPL-2490

UC20-F
426

ION TEMPERATURE BY CHARGE EXCHANGE NEUTRAL ANALY. 'S FROM VERTICAL SIGHTLINES ON THE TOKAMAK FUSION TEST REACTOR

By

C.L. Fiore, S.S. Medley, G.W. Hammett, R. Kaita, and S.D. Scott

DECEMBER 1987

PLASMA
PHYSICS
LABORATORY

PRINCETON UNIVERSITY
PRINCETON, NEW JERSEY

PREPARED FOR THE U.S. DEPARTMENT OF ENERGY,
UNDER CONTRACT DE-AC02-76-CHO-3073.

PPPL--2490

DE88 009351

Ion Temperature by Charge Exchange Neutral Analysis from Vertical Sightlines on the Tokamak Fusion Test Reactor

C.L. Fiore
Plasma Fusion Center, M.I.T.
Cambridge, MA 02139, USA

S.S. Medley, G.W. Hammett, R. Kaita, and S.D. Scott
Plasma Physics Laboratory, Princeton University
Princeton, NJ 08544, USA

Abstract

The Fokker-Planck code FPPRF is used to calculate the expected deuterium charge exchange flux along vertical sightlines from TFTR neutral-beam-injected discharges. The feasibility of obtaining central ion temperature measurements by fitting the spectra obtained from these sightlines at two energy regions–above the highest neutral beam injection energy (> 100 keV) and from 20–80 keV–is investigated. It is demonstrated that the central ion temperature can be obtained from the central vertical sightline by fitting the high energy data. The deuterium neutral particle flux energy distribution below the neutral beam injection energy is insensitive to the code input ion temperature, however.

1. Introduction

Typical energetic ion mode operation on the Tokamak Fusion Test Reactor (TFTR) utilizes deuterium neutral beams injected into a low density deuterium plasma [1]. Measurement of the central ion temperature in these plasmas by charge exchange neutral energy analysis is difficult because the deuterium charge exchange flux is dominated by beam ions [2], which impart the characteristic shape of the neutral beam slowing-down spectrum to the measured neutral energy distribution. In addition, the hydrogen concentration of the plasma is very low, typically $H/(H+D) \sim 1.5\%$, so that there is insufficient neutral hydrogen flux to obtain a spectrum from the thermal background plasma. The purpose of this work is to investigate the nature of the deuterium charge exchange spectra obtained from vertically viewing sightlines by using the Fokker-Planck code FPPRF [3] to calculate the expected charge exchange flux from neutral-beam-injected plasmas. The feasibility of using data from these sightlines to determine the central ion temperature is discussed.

The fast neutral flux obtained from a vertical charge exchange analyzer sightline is derived both from the background thermal plasma and from neutral beam ions which have pitch angle scattered through the appropriate angle. The first goal of this study is to determine whether the deuterium flux from the thermal plasma is sufficiently large compared to the flux arising from the neutral beam ions to be used to obtain the plasma ion temperature. Secondly, application of the technique of fitting the charge exchange neutral energy spectra above the neutral beam injection energy to obtain the central ion temperature, which was demonstrated successfully for data obtained from tangential sightlines [4], is explored for vertical sightlines. A neutral energy spectrum determined from the central vertical chord from a 20 keV ion temperature plasma using the baseline TFTR parameters described in Sec. 2 is shown in Fig. 1. The spectral regions from which the temperature is obtained are the mid-range region, 20–80 keV, and the high energy region, 120–160 keV. The highest neutral beam injection energy is 100 keV.

2. Experimental Conditions used in Simulations

The vertically viewing charge exchange neutral analyzer (CENA) array on TFTR consists of eight separate analyzers, two of which have mass resolving capability. These are positioned in the basement diagnostic area underneath TFTR. The sightlines (Fig. 2) correspond to major radial positions of 1.94 m, 2.08 m, 2.22 m, 2.44 m, 2.7 m, 2.97 m, 3.1 m, and 3.23 m. The analyzers positioned at 2.44 m and 2.97 m are mass resolving.

A TFTR energetic ion mode shot was selected to provide baseline code input parameters for the Fokker-Planck calculations of the charge exchange neutral energy spectra. The plasma has a major radius of 2.45 m and minor radius of 0.8 m. The chosen parameters where $n_e(r) = 7.5\times10^{19}\times(1-r^2/a^2)^4\mathrm{m}^{-3}$, $T_e(r) = 6\times(1-r^2/a^2)$ keV, $T_i = 20\times(1-r^2/a^2)$ keV, $Z_{eff} = 3.5$, $A_{impurity} = 20$, $Z_{impurity} = 10$, $I_{plasma} = 0.85$ MA, $V_{loop} = 0.1$ V, and $B_{toroidal} = 5$ T with 10.5 MW neutral beam power at an energy of 100 keV. The neutral density profile was calculated with the FRANTIC code[5] and is a cylindrically symmetric function of minor radius with a central value of $n_0 = 1.5 \times 10^{12}\mathrm{m}^{-3}$ and an edge value of $n_0 = 5 \times 10^{14}\mathrm{m}^{-3}$. A total neutral beam power of 22 MW was used in the simulations. These baseline parameters are summarized in Table I.

3. The Neutral Energy Spectra from 20–80 keV

The charge exchange neutral flux calculated for the eight vertical sightlines from a 20 keV ion temperature plasma are shown in Figs. 3a and 3b. The characteristic features of the neutral beam slowing-down spectra at 100, 50, and 33 keV corresponding to the full, one-half, and one-third energy components of the neutral beam are apparent.

A comparison of two calculated neutral energy spectra from the central vertical sightline at 2.44 m using 15 and 30 keV input ion temperatures is shown in Fig. 4. It can be seen that the slopes of the spectra in the range of 20–80 keV are extremely similar. The spectra were fit in the energy range of 20–80 keV to obtain a temperature

$$T_{slope} = \left[\frac{d}{dE}\left[ln(\frac{1}{\sqrt{E}}\frac{dn}{dE})\right]\right]^{-1} \tag{1}$$

for each sightline. The results, calculated for input ion temperatures of 15, 20, and 30 keV, are plotted as a function of vertical sightline position in Fig. 5. As is apparent from that figure, the temperature determined from the 20-80 keV region of the neutral energy spectrum is completely insensitive to the input ion temperature.

The particle fraction at each neutral beam energy was varied to test the importance of the neutral beam energy distribution for determining the charge exchange neutral energy distribution. The results are pictured for the 2.44 m sightline in Fig. 6. These cases are for neutral beam current fractions (full, one-half, one-third) of 20:40:40:, 20:50:30, 30:40:30, and 70:15:15. The slope of the spectra in the 20-80 keV range in these cases is determined primarily by the percentage of current in the full energy component of the neutral beam. The slope of the spectra lying above the highest neutral beam injection energy is unaffected by these ratios, however.

Vertical sightline charge exchange spectra were calculated for the cases of all co- and all counter-injection for an input ion temperature of 20 keV with 24 MW neutral beam injection. The temperature calculated from the 20-80 keV energy range as a function of analyzer sightline is shown in Fig. 7. For all sightlines the temperatures determined during co-injection are lower for those with counter-injection, but the difference is very pronounced for the innermost sightlines at 1.94 m and 2.08 m. The input ion temperature was increased to 30 keV for the all counter-injected case, and temperature (again fit from 20–80 keV) as a function of vertical sightline is compared to the same calculation for the 20 keV ion temperature in Fig. 8. Again, there is no sensitivity to input ion temperature.

The lack of dependence on the input ion temperature in the intermediate energy range indicates that fitting the passive deuterium charge exchange spectrum below the highest neutral beam injection energy will not yield a measure of the central ion temperature. Referring again to Fig. 4, note that the slopes of the spectra above the 100 keV neutral beam injection energy are very different for the two cases having input ion temperatures of 15 keV and 30 keV. This suggests that the technique developed earlier for tangential sightlines [4] to derive the ion temperature from the charge exchange spectrum above the neutral beam injection energy can also be applied to the vertical sightlines.

4. The Neutral Energy Spectra above 100 keV

Earlier work for tangential charge exchange analyzer sightlines on TFTR [4] demonstrated that the central ion temperature could be determined from the slope of the charge exchange spectra occurring above the neutral beam injection energy. The temperature, T_{eff}, determined from the slope of the spectrum in that region [as in Eq. (1)] is related to the central ion temperature [6] by

$$T_{eff} = \frac{T_i + (\frac{E}{E_c})^{1.5} T_e}{1 + (\frac{E}{E_c})^{1.5} \pm \tau_s 9.58 \times 10^{11} \frac{Z_b}{A_b} \frac{|\vec{E}^{*}|}{v_b} (\frac{E}{E_c})^{1.5}}. \quad (2)$$

In this equation T_i and T_e are the ion and electron temperatures, Z_b and A_b are the charge and mass of the neutral beam ions, and E_c is the critical energy above which the effects of the electron drag on the beam ions are more important than the ion energy diffusion. E_c is defined as

$$E_c = A_b(\frac{[Z]}{A_i})^{2/3}14.8T_e \tag{3}$$

where

$$\frac{[Z]}{A_i} = \sum \frac{n_i}{n_e}\frac{Z_i^2}{A_i}\frac{ln\Lambda_i}{ln\Lambda_e}. \tag{4}$$

The remaining term in the denominator accounts for the effects of the toroidal electric field, where τ_s is the slowing-down time of the fast ions, v_b is the beam ion velocity, and $|\vec{E}^*| = |\vec{E}|(1 - Z_b/Z_{eff})$ where $|\vec{E}|$ is the magnitude of the electric field in Volts/cm. It was determined in [4] that the electric field term in this equation could be neglected.

T_i determined from T_{eff} as a function of analyzer sightline is shown in Fig. 9 for three values of input ion temperature, 15 keV, 20 keV, and 30 keV. The values of T_i determined for the central sightline at 2.44 m are within 10% of the input value for the three cases shown. However, the error increases rapidly for the noncentral sightlines due to the steepness of the electron temperature gradient outside of the plasma center. The error bars included on the calculated ion temperature are taken from the limits of the electron temperature variation over the width of the radial shell used by the Fokker-Planck code to determine the ion temperature. Even including the uncertainty in the electron temperature in the calculation, the ion temperature determined from noncentral sightlines is higher than the input value. Multiple vertical sightlines are required in actual operation to ensure that a central ion temperature can be obtained when different modes of plasma operation cause the plasma center to be shifted away from the vacuum chamber center.

This calculation was repeated for all co- and all counter-injection cases and the resulting T_i determined from the slope above the neutral beam injection energy is compared to that determined in the baseline case in Fig. 10 for a 20 keV input ion temperature. There is very little difference in the three cases. The value determined from the central sightline agrees very well with the input value, but the noncentral values are all higher than would be expected.

A shell by shell calculation of the charge exchange flux was done in order to determine the spatial origin for the data. The plasma is divided into ten radial shells for the Fokker-Planck calculation, and the contribution to the neutral particle flux is determined individually for each shell. Figure 11 shows the contribution to the flux from the full (100 keV), one-half (50 keV) and, one-third (33 keV) energy components of the neutral beam for the central (2.44 m) sightline. The flux at all three energies increases with radial shell number and peaks in the sixth and seventh shells. Also shown in Fig. 11 is the charge exchange flux calculated at 140 keV as a function of radial shell number. In this case the origin of the flux is peaked for the central four radial shells. This implies that the ion temperature derived from the central vertical sightline above the highest neutral beam injection energy will represent the central ion temperature. However, the charge exchange spectrum below the neutral beam injection energy is derived from $r/a > 0.5$ (corresponding to the fifth and more outboard radial shells).

Figure 12 shows a comparison of the charge exchange spectrum obtained from the central vertical sightline and from a tangential sightline for the same plasma conditions. The calculated flux above the neutral beam injection energy from the vertical sightline is lower than that in the tangential sightline by one e-folding. This indicates that acquiring sufficient signal in the vertical CENA array to measure the central ion temperature from the slope of the distribution function is more difficult than in the tangential case, but is possible.

5. Conclusions

A central ion temperature measurement can be obtained from the charge exchange data collected from the vertical CENA array on TFTR by fitting the central sightline data at energies higher than the neutral beam injection energy. The Fokker-Planck calculation of the neutral particle flux at high energy gives an energy spectrum which is consistent with the input ion temperature, and which arises from the plasma center. The spectra calculated for noncentral sightlines result in an inconsistently high value compared to the input ion temperature for those sightlines, however.

Fitting the calculated vertical sightline neutral energy spectra at energies below the neutral beam injection energy leads to ion temperature values which are not sensitive to the input ion temperature for the calculations. The spectrum in this energy region (20-80 keV) is primarily sensitive to the distribution of neutral beam particles between the full, one-half, and, one-third energy components. An ion temperature cannot be derived from the vertical sightline deuterium data below the neutral beam injection energy.

Acknowledgments

The authors gratefully acknowledge K. M. Young, L. C. Johnson, and the entire TFTR group for their support of this work. This work was sponsored by the United States Department of Energy under Contract DE-AC02-78ET51013 and Contract DE-AC02-76CHO3073.

References

[1]STRACHAN, J.D., BITTER, M., RAMSEY, A.T., ZARNSTORFF, M.C., ARUNASALAM, V., *et al.*, Phys. Rev. Lett. **58** (1987) 1004.

[2]DAVIS, S.L., MUELLER, D., KEANE, C.J., Rev. Sci. Instrum. **54** (1983) 315.

[3]HAMMETT, G.W., "Fast Ion Studies of Ion Cyclotron Heating in the PLT Tokamak," PhD Thesis, Princeton University (1986); also GOLDSTON, R.J., "Fast Ion Diagnostic Experiment on ATC: Radially Resolved Measurements of q, Z_{eff}, $T_{i\parallel}$,and $T_{i\nparallel}$," PhD Thesis, Princeton University (1977); also CORDEY, J.G., Nucl. Fusion **16** (1976) 499.

[4]FIORE, C.L., MEDLEY, S. S., HAMMETT, G.W., KAITA, R., ROQUEMORE, A.L., SCOTT, S.D., "Ion Temperature from Tangential Charge Exchange Neutral Analysis on the Tokamak Fusion Test Reactor," Princeton Plasma Physics Laboratory Report No. PPPL-2476. Nucl. Fusion (to be published).

[5]TAMOR, S.J., J. Comput. Phys. **40** (1981) 104.

[6]GOLDSTON, R.J., "Fast Ion Diagnostic Experiment on ATC: Radially Resolved Measurements of q, Z_{eff}, $T_{i\parallel}$,and $T_{i\nparallel}$," PhD. Thesis, Princeton University (1977). A factor of $1/v_b$ in the electric field term inadvertently omitted in Eq. (29) has been included in our Eq. (1).

Table Ia. Plasma Parameters Used in the Simulations

TFTR High Ion Energy Mode Baseline Shot Based on #26608

$T_e(r) = T_{e0} \times (1 - r^2/a^2)^2$ keV, $T_{e0} = 6$ keV

$T_i(r) = T_{i0} \times (1 - r^2/a^2)^2$ keV, $T_{i0} = 20$ keV

$n_e = n_{e0} \times (1 - r^2/a^2)^4$, $n_{e0} = 7.5 \times 10^{19}\text{m}^{-3}$

$P_{beam} = 10.5$ MW (22 MW used in simulations)

$E_{beam} = 100$ keV

$Z_{eff} = 3.5$

$A_{imp} = 20$

$Z_{imp} = 10$

$n_0(r/a = 0) = 1.5 \times 10^{12}\text{m}^{-3}$, $n_0(r/a = 1) = 5.5 \times 10^{14}\text{m}^{-3}$, FRANTIC profile

$B_{toroidal} = 5.1$ T

$I_{plasma} = 0.85$ MA

$V_{loop} = 0.1$ V

Table Ib. Neutral Beam Injection Tangency Radii used in Simulations

Baseline:

Beam	Radius	Power
2A	-1.73 m	2MW
2B	-1.99	2
2C	-2.23	2
3A	2.53	2
3B	2.31	2
3C	2.07	2
4A	2.84	2
4B	2.63	2
4C	2.41	2
5A	2.23	2
5C	1.75	2

All co:

Radius	Power
2.25 m	8 MW
2.0	8
1.75	8

All counter:

Radius	Power
-1.75 m	8 MW
-2.0	8
-2.25	8

Figure Captions

Figure 1. Fokker-Planck calculation of the deuterium charge exchange neutral spectrum from the 2.44 m vertical sightline during deuterium neutral beam injection for a baseline energetic ion mode discharge. $T_i = 20$ keV, $T_e = 6$ keV, $n_e = 7.5 \times 10^{19}(1 - r^2/a^2)^4 \mathrm{m}^{-3}$, $Z_{eff} = 3.5$, $I_{plasma} = 0.85$ MA, $P_{beam} = 22$ MW, $B_{toroidal} = 5.5$ T, $V_l = 0.11$ V. The ion temperature will be derived from the slope of the distribution function in the mid-range, 20–80 keV and above the highest neutral beam injection energy, 120–160 keV.

Figure 2. Orientation of the vertical CENA sightlines on TFTR. The plasma major radius is R_0 =2.45 m. Simulations were done for each of the CENA sightlines at major radial positions of 1.94 m, 2.08 m, 2.22 m, 2.44 m, 2.70 m, 2.97 m, 3.10 m, and 3.23 m.

Figure 3. Fokker-Planck calculation of the deuterium charge exchange neutral spectrum from the vertical sightlines a) at 1.94 m, 2.08 m, 2.22 m, and 2.44 m and from the vertical sightlines b) at 2.70 m, 2.97 m, 3.10 m, and 3.23 m during deuterium neutral beam injection for a baseline energetic ion mode discharge. $T_i = 20$ keV, $T_e = 6$ keV, $n_e = 7.5\times 10^{19}(1-r^2/a^2)^4 \mathrm{m}^{-3}$, $Z_{eff} = 3.5$, $I_{plasma} = 0.85$ MA, $P_{beam} = 22$ MW, $B_{toroidal} = 5.5$ T, $V_l = 0.11$ V.

Figure 4. Fokker-Planck calculation of the deuterium charge exchange neutral spectrum from the 2.44 m (central) vertical sightline for input ion temperatures of 15 keV and 30 keV during deuterium neutral beam injection for a baseline energetic ion mode discharge. $T_e = 6$ keV, $n_e = 7.5 \times 10^{19}(1 - r^2/a^2)^4 \mathrm{m}^{-3}$, $Z_{eff} = 3.5$, $I_{plasma} = 0.85$ MA, $P_{beam} = 22$ MW, $B_{toroidal} = 5.5$ T, $V_l = 0.11$ V.

Figure 5. T_i derived from the slope of the calculated charge exchange spectrum in the energy range 20–80 keV for input ion temperatures of 15 keV, 20 keV, and 30 keV during deuterium neutral beam injection. As the data clearly indicate, the 20-80 keV range of the charge exchange spectrum is insensitive to the bulk plasma ion temperature. All other parameters are those of the baseline energetic ion mode discharge. $T_e = 6$ keV, $n_e = 7.5 \times 10^{19}(1 - r^2/a^2)^4 \mathrm{m}^{-3}$, $Z_{eff} = 3.5$, $I_{plasma} = 0.85$ MA, $P_{beam} = 22$ MW, $B_{toroidal} = 5.5$ T, $V_l = 0.11$ V.

Figure 6. Fokker-Planck calculation of the deuterium charge exchange neutral spectrum from the 2.44 m (central) vertical sightline for different neutral beam current fractions dur-

ing deuterium neutral beam injection for a baseline energetic ion mode discharge. The spectra are for energy distributions of (full: one-half: one-third) 70:15:15, 30:40:30, 20:50:30, and 20:40:40. $T_i = 20$ keV, $T_e = 6$ keV, $n_e = 7.5 \times 10^{19}(1 - r^2/a^2)^4\mathrm{m}^{-3}$, $Z_{eff} = 3.5$, $I_{plasma} = 0.85$ MA, $P_{beam} = 22$ MW, $B_{toroidal} = 5.5$ T, $V_l = 0.11$ V.

Figure 7. T_i derived from the slope of the calculated charge exchange spectrum in the energy range 20–80 keV for all co- and all counter deuterium neutral beam injection. All other parameters are those of the baseline energetic ion mode discharge. $T_i = 20$ keV, $T_e = 6$ keV, $n_e = 7.5 \times 10^{19}(1 - r^2/a^2)^4\mathrm{m}^{-3}$, $Z_{eff} = 3.5$, $I_{plasma} = 0.85$ MA, $P_{beam} = 24$ MW, $B_{toroidal} = 5.5$ T, $V_l = 0.11$ V.

Figure 8. T_i derived from the slope of the calculated charge exchange spectrum in the energy range 20–80 keV for all counter deuterium neutral beam injection for input ion temperatures of 20 keV and 30 keV. All other parameters are those of the baseline energetic ion mode discharge. $T_e = 6$ keV, $n_e = 7.5\times10^{19}(1-r^2/a^2)^4\mathrm{m}^{-3}$, $Z_{eff} = 3.5$, $I_{plasma} = 0.85$ MA, $P_{beam} = 24$ MW, $B_{toroidal} = 5.5$ T, $V_l = 0.11$ V.

Figure 9. T_i calculated from T_{eff} (the inverse of the slope of the deuterium charge exchange spectrum above the highest neutral beam injection energy) as a function of vertical sightline for input ion temperatures of 15 keV, 20 keV, and 30 keV. The error bars reflect the variation in the electron temperature over the width of the Fokker-Planck shell used to calculate the neutral particle spectra. All other parameters are from the TFTR energetic ion mode baseline discharge.

Figure 10. T_i calculated from T_{eff} as a function of vertical sightline for all co-injection, all counter-injection, and for the baseline case for an input ion temperatures of 20 keV. All other parameters are from the TFTR energetic ion mode baseline discharge.

Figure 11. Calculated neutral particle efflux from the plasma for the 2.44 m vertical sightline as a function of Fokker-Planck shell for the full (100 keV), one-half (50 keV), and one-third (33 keV) neutral beam energy components (open data points). The flux is peaked in shells 5–7. The flux at 140 keV is peaked in the center 4 shells (solid data points). All parameters are from the TFTR energetic ion mode baseline discharge. $T_i = 20$ keV, $T_e = 6$ keV, $n_e = 7.5 \times 10^{19}(1 - r^2/a^2)^4\mathrm{m}^{-3}$, $Z_{eff} = 3.5$, $I_{plasma} = 0.85$ MA, $P_{beam} = 22$ MW, $B_{toroidal} = 5.5$ T, $V_l = 0.11$ V.

Figure 12. Fokker-Planck calculation of the deuterium charge exchange neutral spectrum from the 2.0 m tangential sightline compared to that from the 2.44 m vertical sightline during deuterium neutral beam injection for a baseline energetic ion mode discharge. T_i = 20 keV, T_e = 6 keV, $n_e = 7.5 \times 10^{19}(1 - r^2/a^2)^4 \mathrm{m}^{-3}$, Z_{eff} = 3.5, I_{plasma} = 0.85 MA, P_{beam} = 22 MW, $B_{toroidal}$ = 5.5 T, V_l = 0.11 V. T_i calculated for the vertical view compares favorably with that obtained in the tangential case.

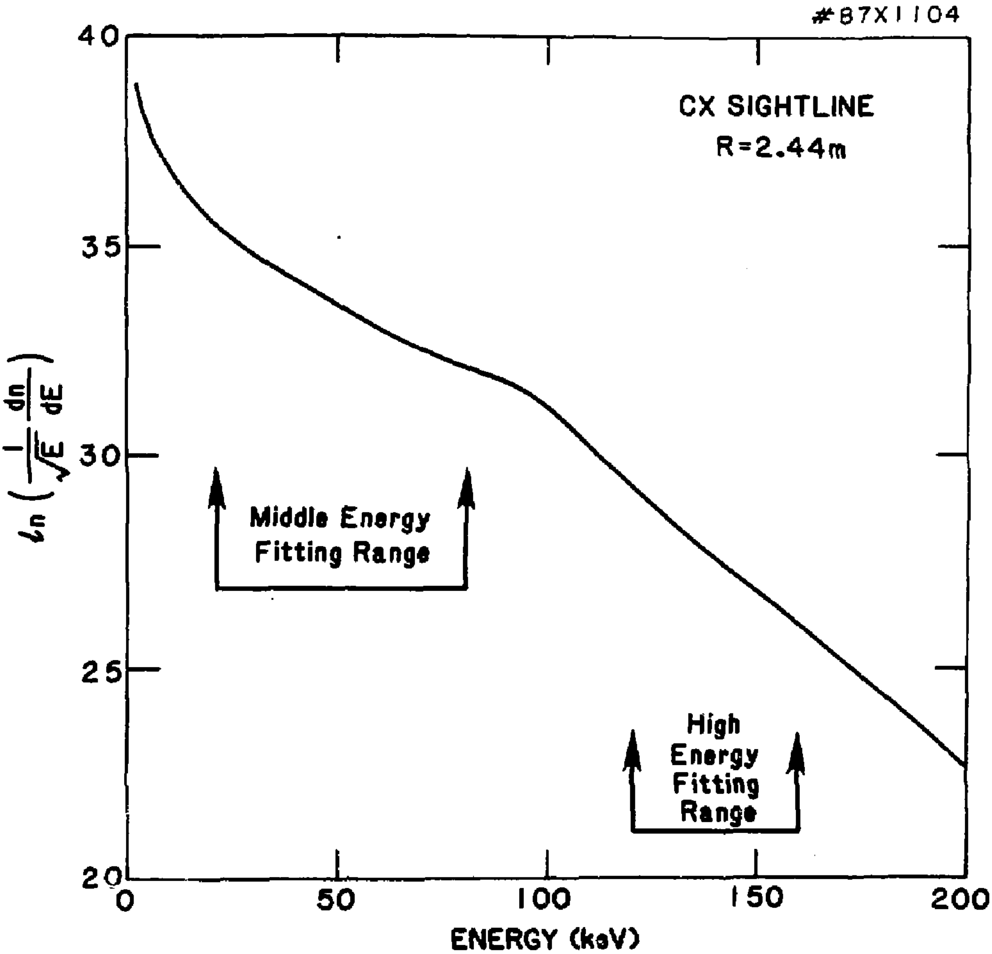
#87X1104
CX SIGHTLINE
R=2.44m
Middle Energy
Fitting Range
High
Energy
Fitting
Range
40
35
30
25
20
0
50
100
150
200
ENERGY (keV)
ln (1/√E dn/dE)

Fig. 1

#87X1095

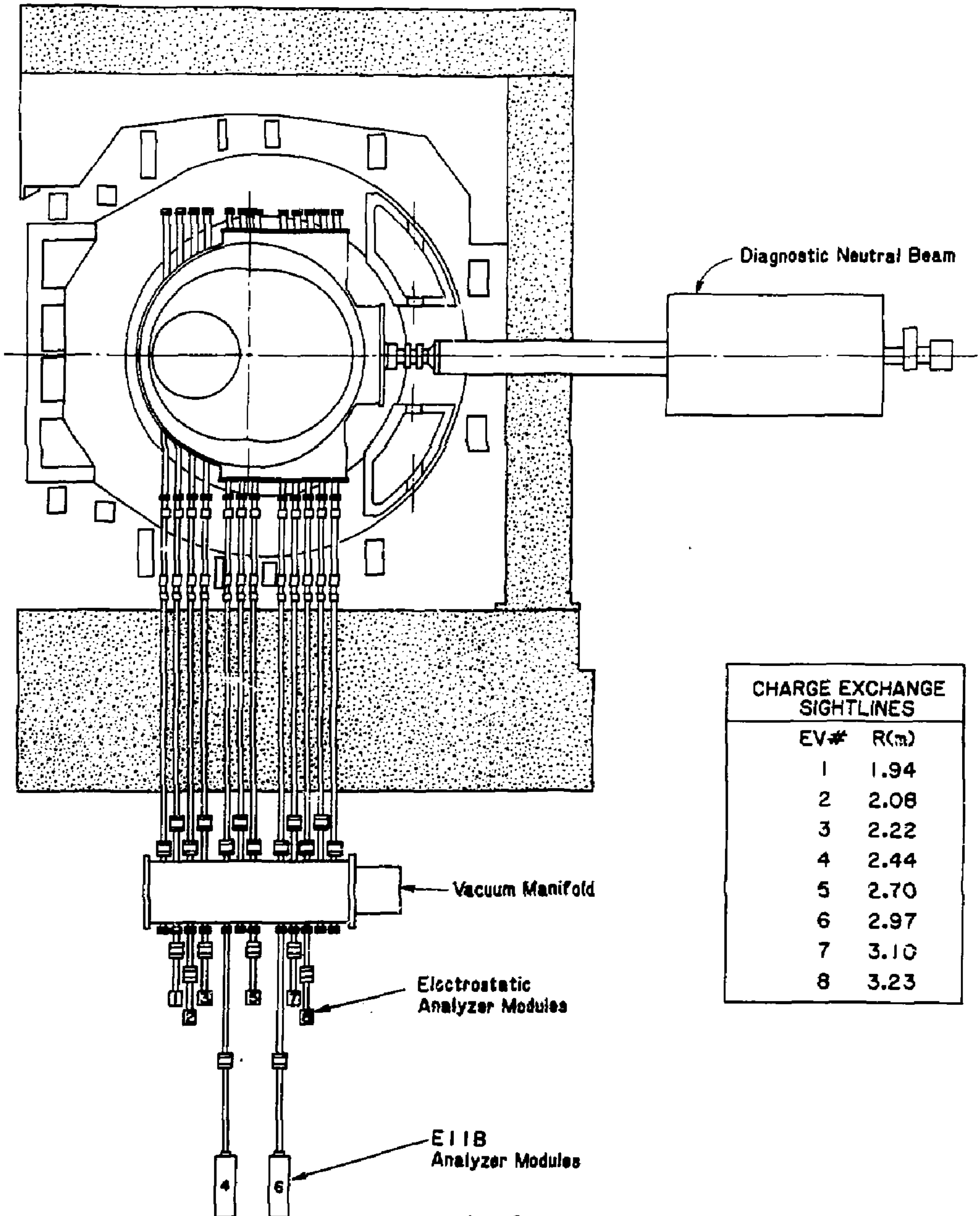

CHARGE EXCHANGE SIGHTLINES	
EV#	R(m)
1	1.94
2	2.08
3	2.22
4	2.44
5	2.70
6	2.97
7	3.10
8	3.23

Fig. 2

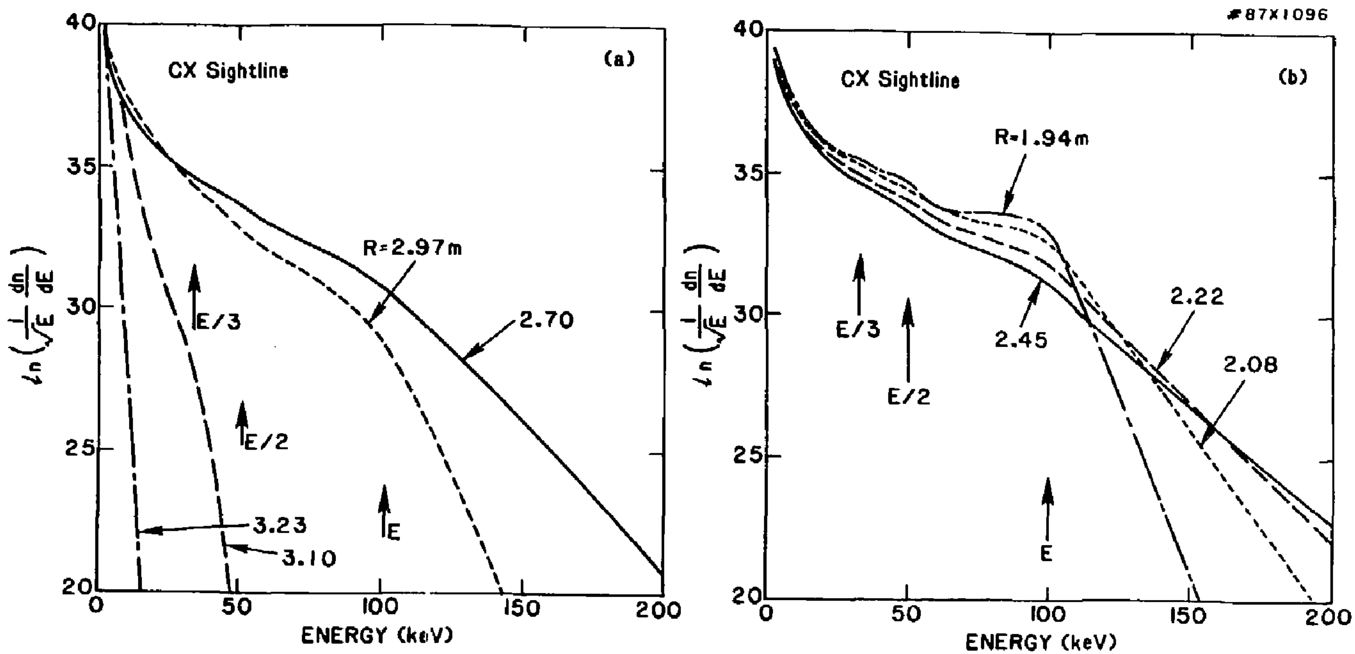

#87X1096
CX Sightline
(a)
R=2.97m
2.70
3.23
3.10
E/3
E/2
E
ENERGY (keV)
CX Sightline
(b)
R=1.94m
2.22
2.45
2.08
E/3
E/2
E
ENERGY (keV)

Fig. 3

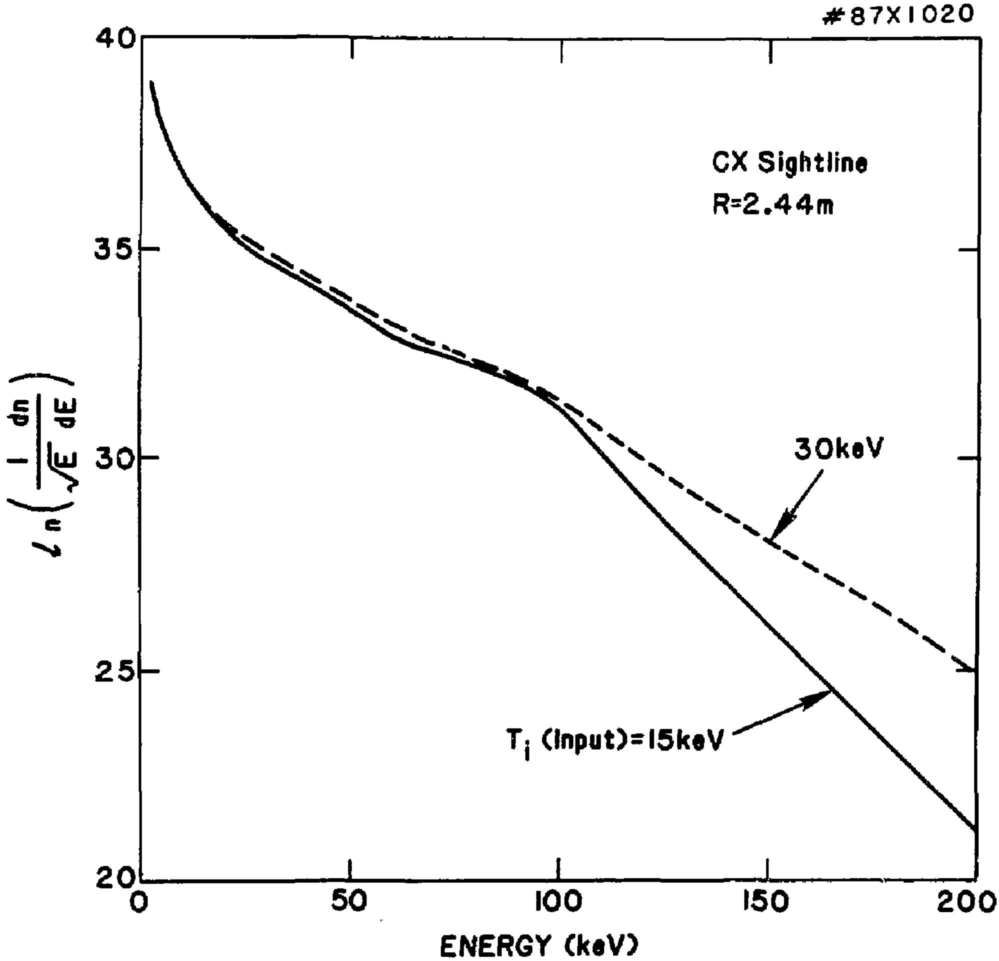
#87X1020
CX Sightline
R=2.44m
30keV
T_i (Input)=15keV
40
35
30
25
20
0
50
100
150
200
ENERGY (keV)
ℓn(1/√E dn/dE)

Fig. 4

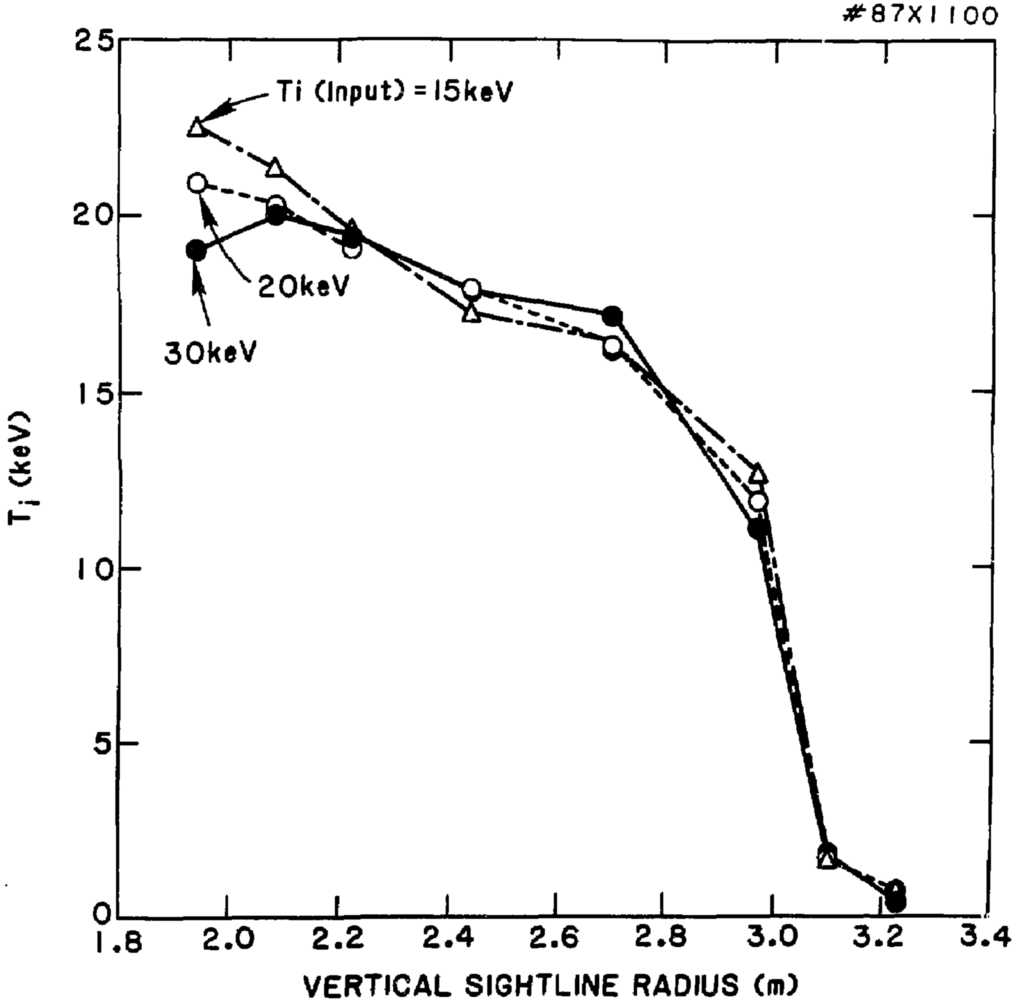

#87X1100
Ti (Input) = 15keV
20keV
30keV
25
20
15
10
5
0
Ti (keV)
1.8
2.0
2.2
2.4
2.6
2.8
3.0
3.2
3.4
VERTICAL SIGHTLINE RADIUS (m)

Fig. 5

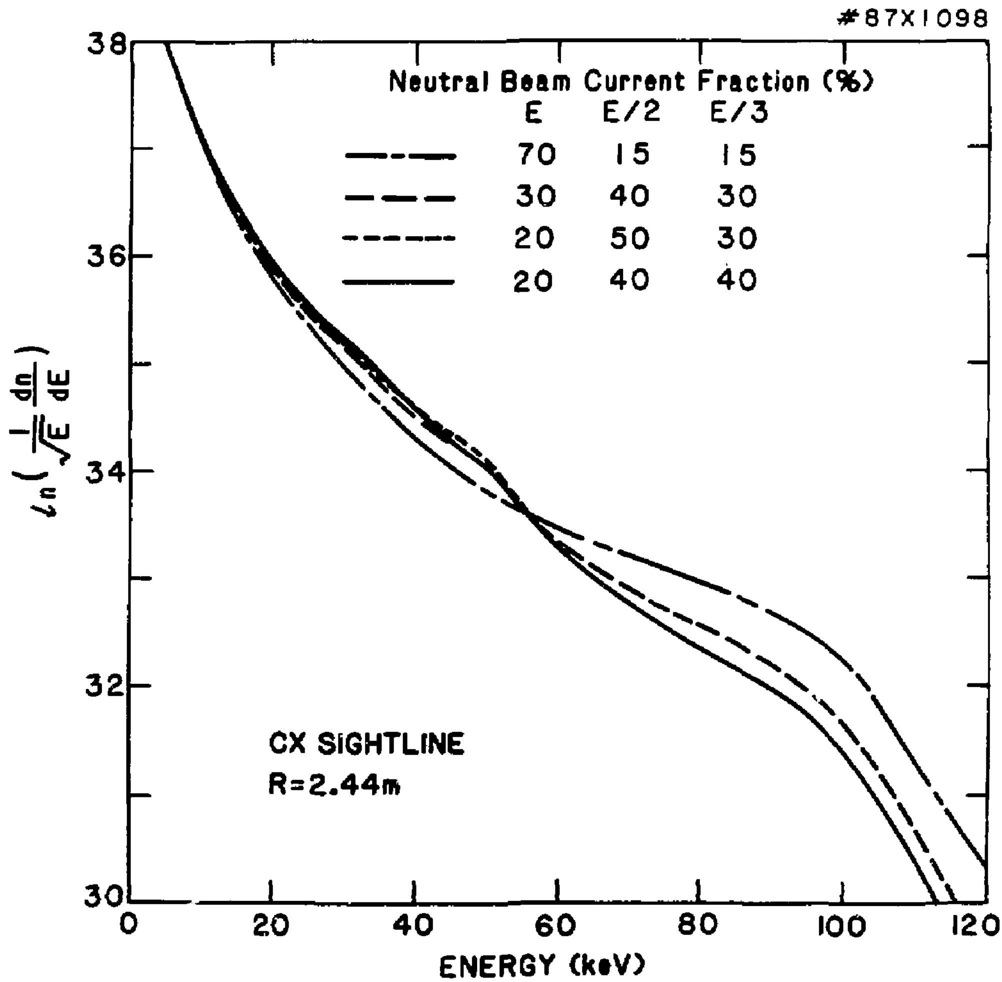
#87X1098
Neutral Beam Current Fraction (%)
E E/2 E/3
70 15 15
30 40 30
20 50 30
20 40 40
CX SIGHTLINE
R=2.44m
38
36
34
32
30
0
20
40
60
80
100
120
ENERGY (keV)
ln(1/√E dn/dE)

Fig. 6

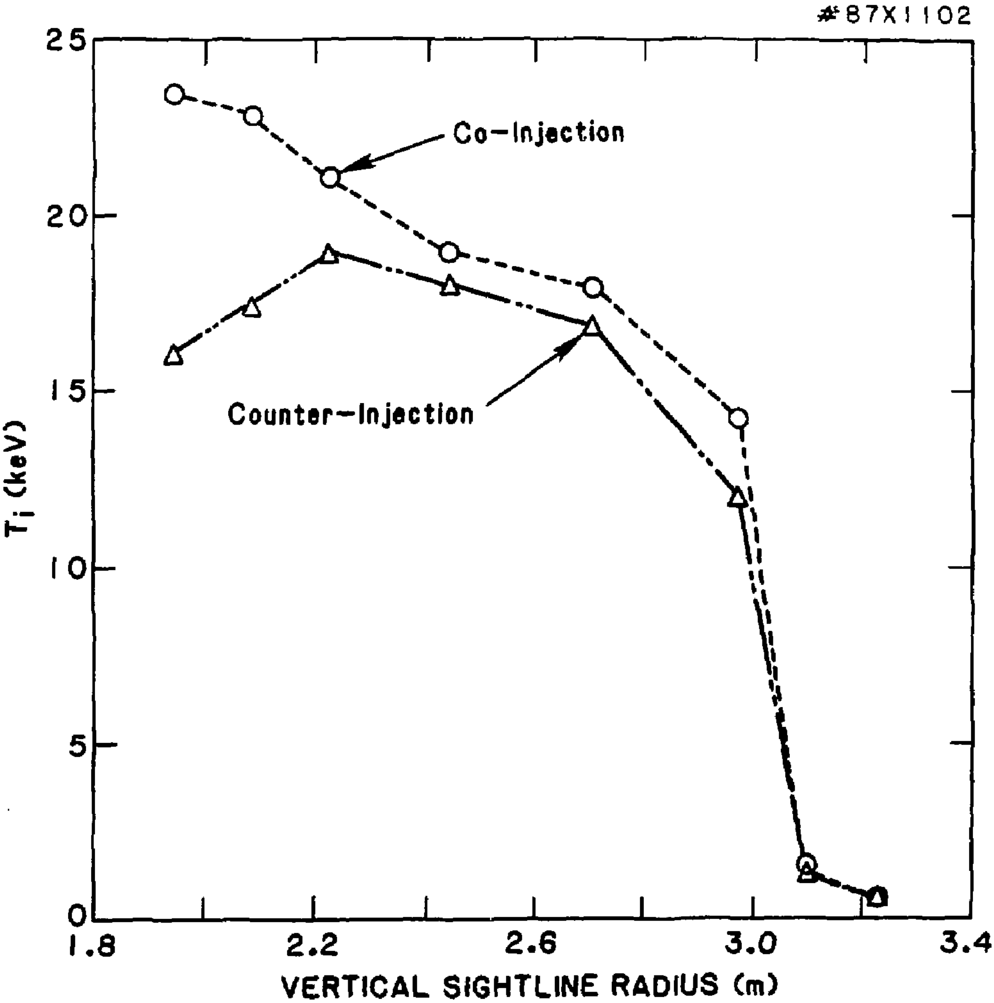
#87X1102
25
20
15
10
5
0
1.8
2.2
2.6
3.0
3.4
Co-Injection
Counter-Injection
T_i (keV)
VERTICAL SIGHTLINE RADIUS (m)

Fig. 7

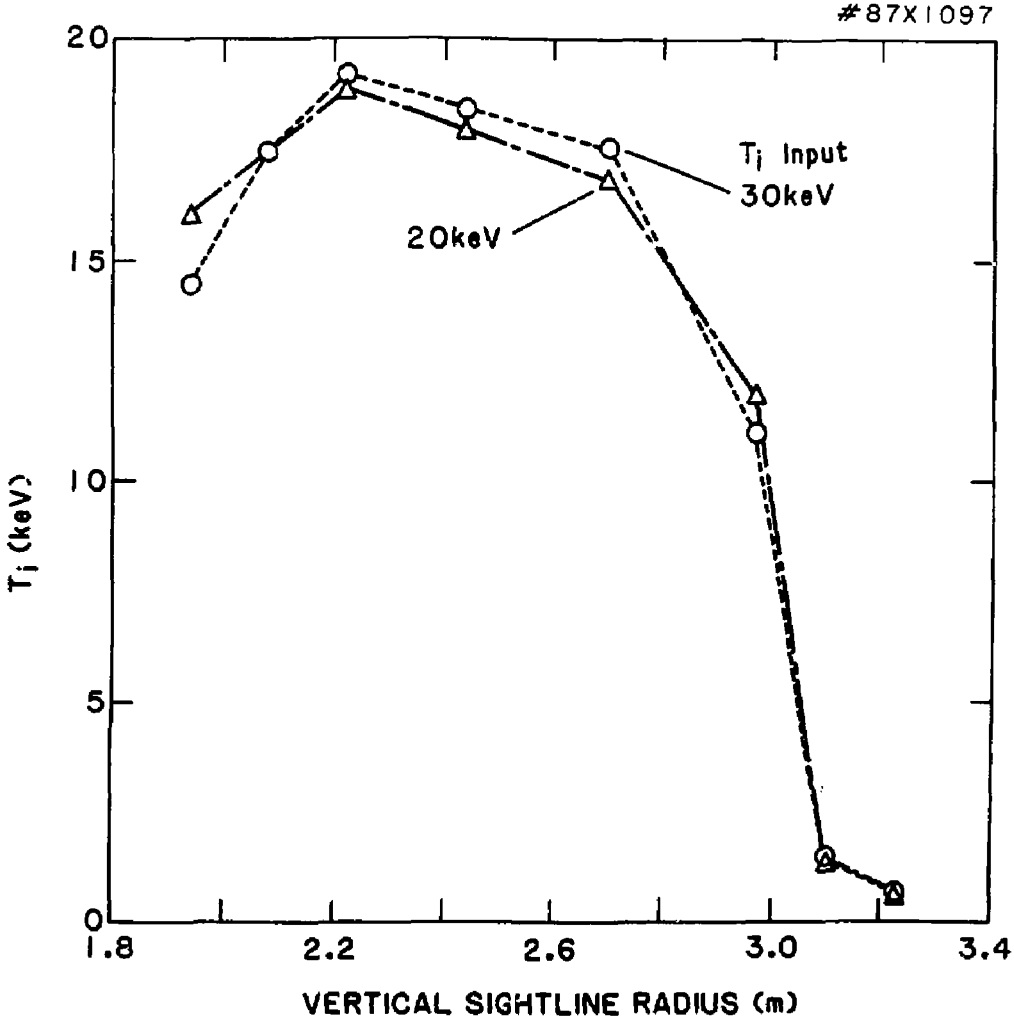

#87X1097
20
15
10
5
0
1.8
2.2
2.6
3.0
3.4
T_i (keV)
VERTICAL SIGHTLINE RADIUS (m)
T_i Input
30keV
20keV

Fig. 8

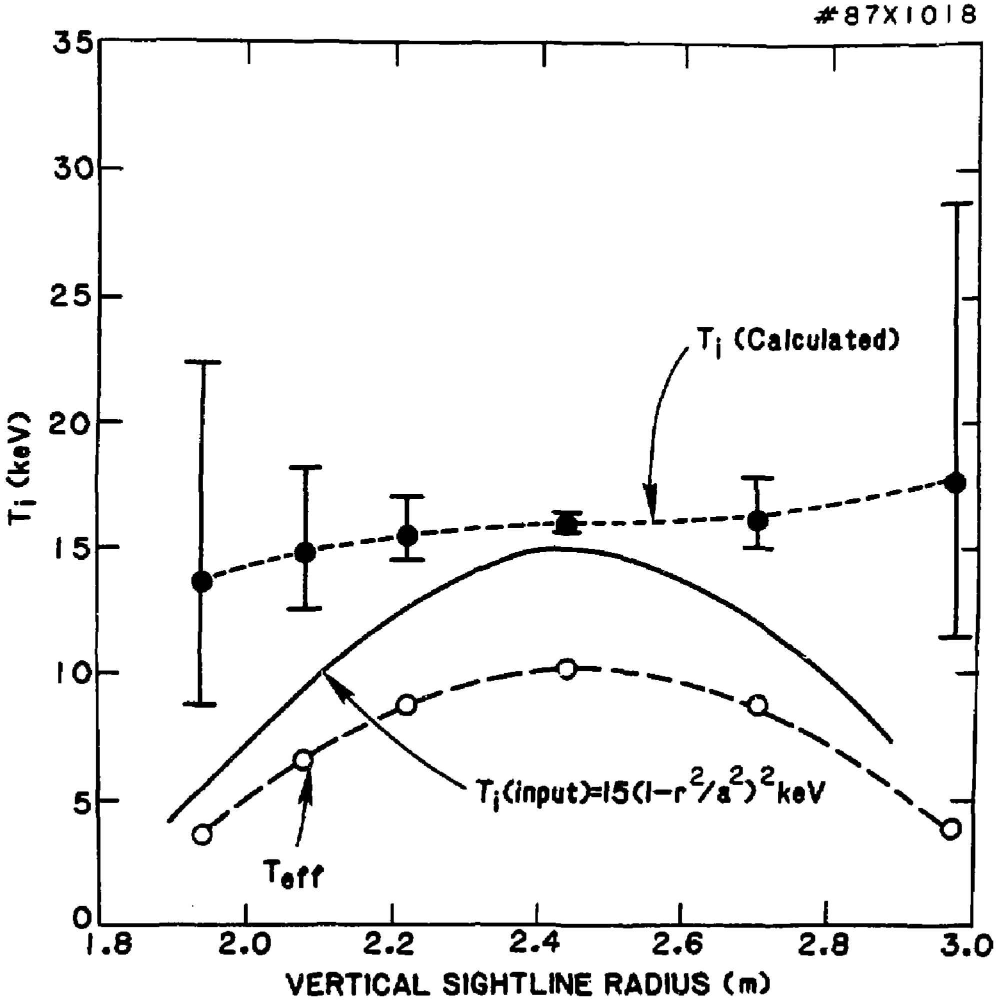
#87X1018
35
30
25
20
15
10
5
0
Ti (keV)
Ti (Calculated)
Ti(input)=15(1−r²/a²)²keV
Teff
1.8
2.0
2.2
2.4
2.6
2.8
3.0
VERTICAL SIGHTLINE RADIUS (m)

Fig. 9a

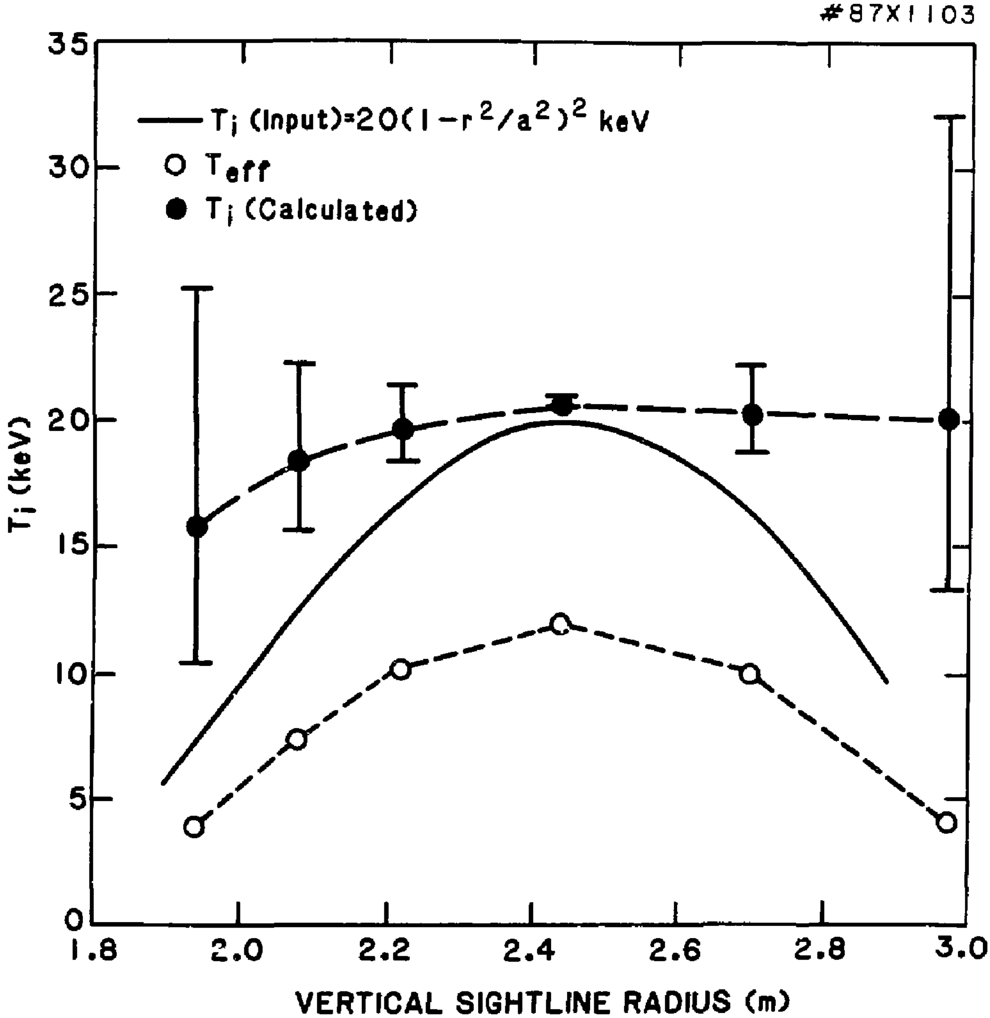
#87X1103
T_i (Input)=20(1−r²/a²)² keV
T_{eff}
T_i (Calculated)
T_i (keV)
35
30
25
20
15
10
5
0
1.8
2.0
2.2
2.4
2.6
2.8
3.0
VERTICAL SIGHTLINE RADIUS (m)

Fig. 9b

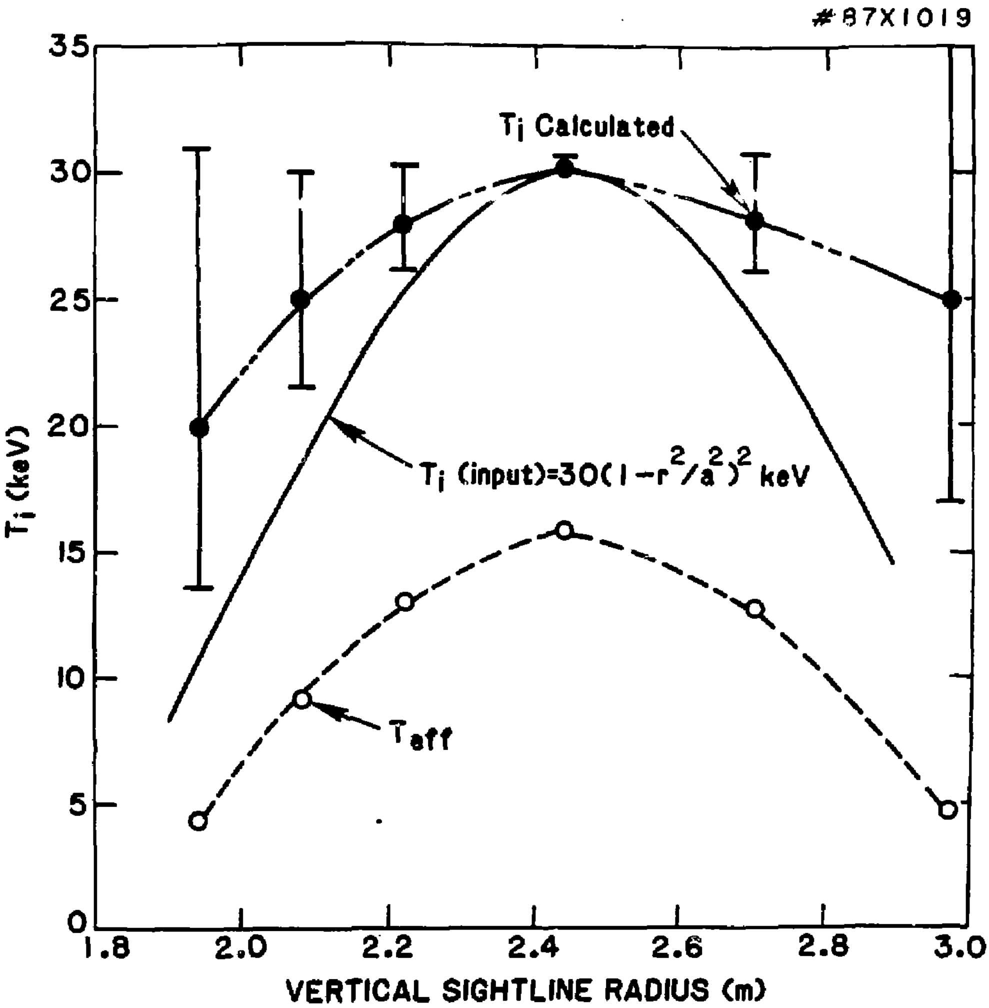
#87X1019
35
30
25
20
15
10
5
0
1.8
2.0
2.2
2.4
2.6
2.8
3.0
VERTICAL SIGHTLINE RADIUS (m)
Ti (keV)
Ti Calculated
Ti (input)=30(1-r2/a2)2 keV
Teff

Fig. 9c

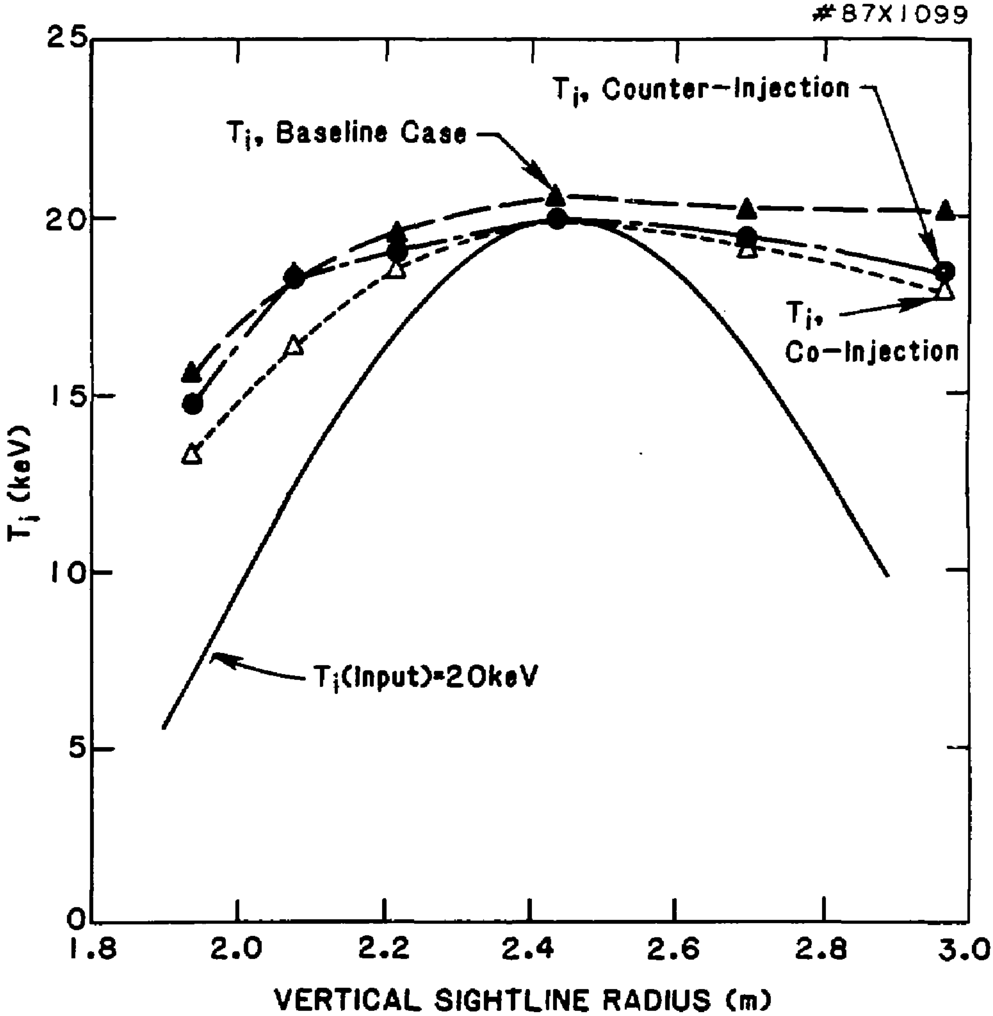
#87X1099
Tᵢ, Counter–Injection
Tᵢ, Baseline Case
Tᵢ, Co–Injection
Tᵢ(Input)=20keV
Tᵢ (keV)
VERTICAL SIGHTLINE RADIUS (m)
25
20
15
10
5
0
1.8
2.0
2.2
2.4
2.6
2.8
3.0

Fig. 10

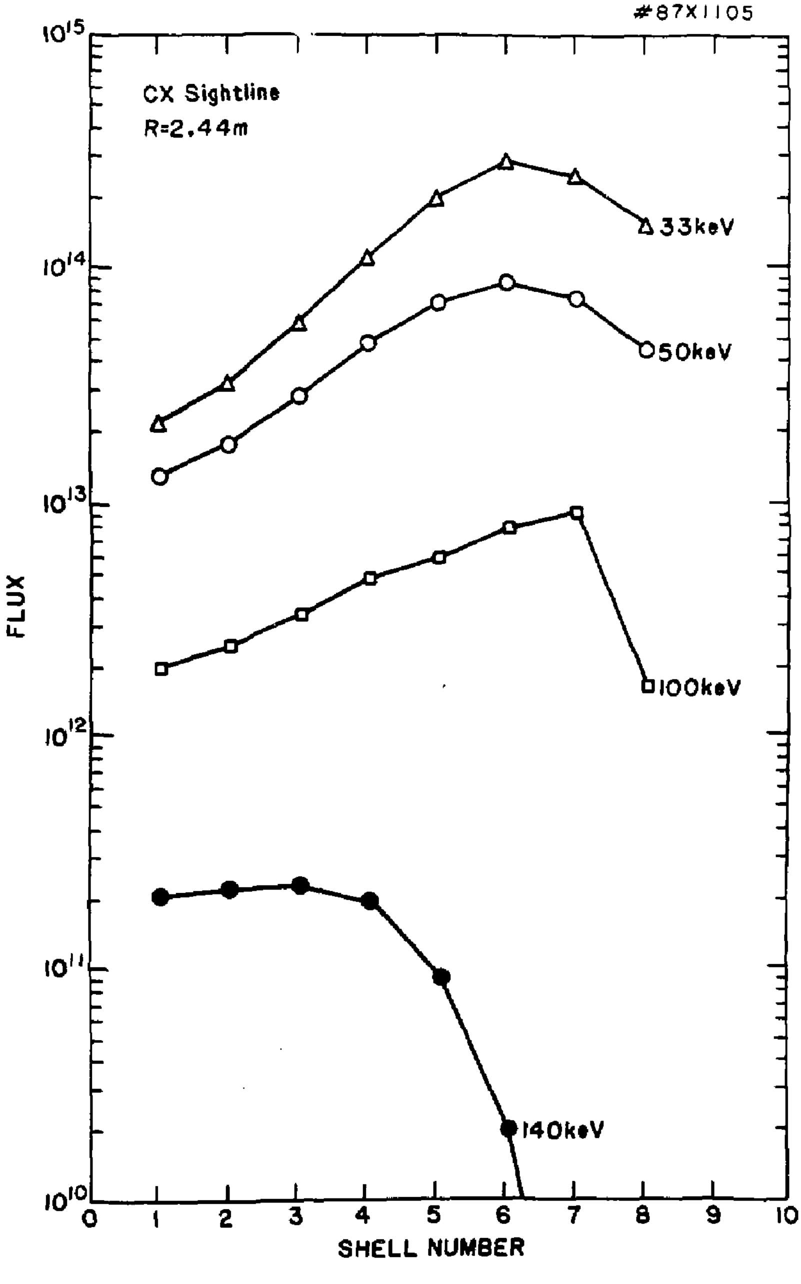

#87X1105
CX Sightline
R=2.44m
33keV
50keV
100keV
140keV
FLUX
SHELL NUMBER

Fig. 11

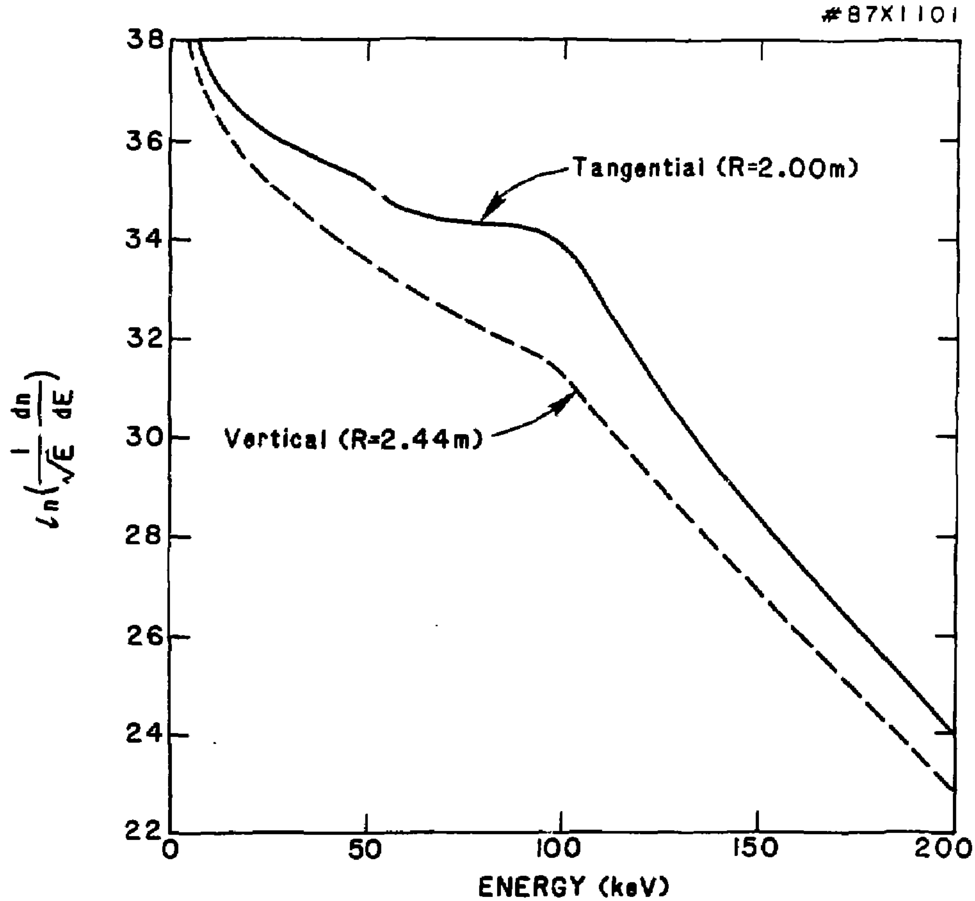
#87X1101
38
36
34
32
30
28
26
24
22
0
50
100
150
200
ENERGY (keV)
ln(1/√E dn/dE)
Tangential (R=2.00m)
Vertical (R=2.44m)

Fig. 12

EXTERNAL DISTRIBUTION IN ADDITION TO UC-20

Dr. Frank J. Paoloni, Univ of Wollongong, AUSTRALIA
Prof. M.H. Brennan, Univ Sydney, AUSTRALIA
Plasma Research Lab., Australian Nat. Univ., AUSTRALIA
Prof. I.R. Jones, Flinders Univ., AUSTRALIA
Prof. F. Cap, Inst Theo Phys, AUSTRIA
Prof. M. Heindler, Institut fur Theoretische Physik, AUSTRIA
M. Goossens, Astronomisch Instituut, BELGIUM
Ecole Royale Militaire, Lab de Phys Plasmas, BELGIUM
Commission-European, Dg-XII Fusion Prog, BELGIUM
Prof. R. Boucique, Laboratorium voor Natuurkunde, BELGIUM
Dr. P.H. Sakanaka, Instituto Fisica, BRAZIL
Instituto De Pesquisas Espaciasi-INPE, BRAZIL
Documents Office, Atomic Energy of Canada Limited, CANADA
Dr. M.P. Bachynski, MPB Technologies, Inc., CANADA
Dr. H.M. Skarsgard, University of Saskatchewan, CANADA
Dr. H. Barnard, University of British Columbia, CANADA
Prof. J. Teichmann, Univ. of Montreal, CANADA
Prof. S.R. Sreenivasan, University of Calgary, CANADA
Prof. Tudor W. Johnston, INRS-Energie, CANADA
Dr. C.R. James, Univ. of Alberta, CANADA
Dr. Peter Lukac, Komenskeho Univ, CZECHOSLOVAKIA
The Librarian, Culham Laboratory, ENGLAND
The Librarian, Rutherford Appleton Laboratory, ENGLAND
Mrs. S.A. Hutchinson, JET Library, ENGLAND
C. Mouttet, Lab. de Physique des Milieux Ionisés, FRANCE
J. Radet, CEN/CADARACHE - Bat 506, FRANCE
Univ. of Ioannina, Library of Physics Dept. GREECE
Dr. Tom Mual, Academy Bibliographic Ser., HONG KONG
Preprint Library, Hungarian Academy of Sciences, HUNGARY
Dr. B. Dasgupta, Saha Inst of Nucl. Phys., INDIA
Dr. P. Kaw, Institute for Plasma Research, INDIA
Dr. Philip Rosenau, Israel Inst. Tech, ISRAEL
Librarian, Int'l Ctr Theo Phys, ITALY
Prof. G. Rostagni, Univ Di Padova, ITALY
Miss Clelia De Palo, Assoc EURATOM-ENEA, ITALY
Biblioteca, Instituto di Fisica del Plasma, ITALY
Dr. H. Yamato, Toshiba Res & Dev, JAPAN
Prof. I. Kawakami, Atomic Energy Res. Institute, JAPAN
Prof. Kyoji Nishikawa, Univ of Hiroshima, JAPAN
Direc. Dept. Large Tokamak Res. JAERI, JAPAN
Prof. Satoshi Itoh, Kyushu University, JAPAN
Research Info Center, Nagoya University, JAPAN
Prof. S. Tanaka, Kyoto University, JAPAN
Library, Kyoto University, JAPAN
Prof. Nobuyuki Inoue, University of Tokyo, JAPAN
S. Mori, JAERI, JAPAN
Librarian, Korea Advanced Energy Res. Institute, KOREA
Prof. D.I. Choi, Adv. Inst Sci & Tech, KOREA
Prof. B.S. Liley, University of Waikato, NEW ZEALAND
Institute of Plasma Physics, PEOPLE'S REPUBLIC OF CHINA
Librarian, Institute of Phys., PEOPLE'S REPUBLIC OF CHINA
Library, Tsing Hua University, PEOPLE'S REPUBLIC OF CHINA
Z. Li, Southwest Inst. Physics, PEOPLE'S REPUBLIC OF CHINA
Prof. J.A.C. Cabral, Inst Superior Tecnico, PORTUGAL
Dr. Octavian Petrus, AL I CUZA University, ROMANIA
Dr. Johan de Villiers, Fusion Studies, AEC, SO AFRICA
Prof. M.A. Hellberg, University of Natal, SO AFRICA
C.I.E.M.A.T., Fusion Div. Library, SPAIN
Dr. Lennart Stenflo, University of UMEA, SWEDEN
Library, Royal Inst Tech, SWEDEN
Prof. Hans Wilhelmson, Chalmers Univ Tech, SWEDEN
Centre Phys des Plasmas, Ecole Polytech Fed, SWITZERLAND
Bibliotheek, Fom-Inst Voor Plasma-Fysica, THE NETHERLANDS
Dr. D.D. Ryutov, Siberian Acad Sci, USSR
Dr. G.A. Eliseev, Kurchatov Institute, USSR
Dr. V.A. Glukhikh, Inst Electrophysical Apparatus, USSR
Dr. V.T. Tolok, Inst. Phys. Tech. USSR
Dr. L.M. Kovrizhnykh, Institute Gen. Physics, USSR
Nuclear Res. Establishment, Julich Ltd., W. GERMANY
Bibliothek, Inst. Fur Plasmaforschung, W. GERMANY
Dr. K. Schindler, Ruhr Universitat Bochum, W. GERMANY
ASDEX Reading Rm, IPP/Max-Planck-Institut fur Plasmaphysik, W. GERMANY
Librarian, Max-Planck Institut, W. GERMANY
Prof. R.K. Janev, Inst Phys, YUGOSLAVIA